Advances in Applied Mathematics and Mechanics
Adv. Appl. Math. Mech., Vol. **13**, No. 6, pp. 1384-1397

DOI: 10.4208/aamm.OA-2020-0317
December 2021

An ADI Sparse Grid method for Pricing Efficiently American Options under the Heston Model

A. Clevenhaus*, M. Ehrhardt and M. Günther

Institute of Mathematical Modelling, Analysis and Computational Mathematics (IMACM), Chair of Applied Mathematics and Numerical Analysis, Bergische Universität Wuppertal, Gaußstraße 20, 42119 Wuppertal, Germany

Received 13 October 2020; Accepted (in revised version) 9 March 2021

Abstract. One goal of financial research is to determine fair prices on the financial market. As financial models and the data sets on which they are based are becoming ever larger and thus more complex, financial instruments must be further developed to adapt to the new complexity, with short runtimes and efficient use of memory space. Here we show the effects of combining known strategies and incorporating new ideas to further improve numerical techniques in computational finance.

In this paper we combine an ADI (alternating direction implicit) scheme for the temporal discretization with a sparse grid approach and the combination technique. The later approach considerably reduces the number of "spatial" grid points. The presented standard financial problem for the valuation of American options using the Heston model is chosen to illustrate the advantages of our approach, since it can easily be adapted to other more complex models.

AMS subject classifications: 65M10, 78A48

Key words: Sparse grid, combination technique, American options, ADI, Heston model.

1 Introduction

A fair price of a financial derivative is arbitrage-free, which means that the price does not guarantee a profit. A financial derivative is a contract between parties whose value at the maturity date T is determined by the underlying assets at the time T or before the time T. Options are a special type of financial derivative.

A plain vanilla option is a contract that gives the holder the right (but not the obligation) to exercise a particular transaction at time T or until time T at a fixed price K (strike). We distinguish between call and put options. A call option holder has the right to buy

*Corresponding author.
Emails: clevenhaus@uni-wuppertal.de (A. Clevenhaus), ehrhardt@uni-wuppertal.de (M. Ehrhardt), guenther@uni-wuppertal.de (M. Günther)

from the writer, and if a put option is held, the holder has the right to sell it to the writer. The time of exercise defines the type of option: if the holder has the right to exercise the option only on a certain predefined expiration date T, a European option is used, whereas if the holder can exercise at any time before and at maturity T, an American option is considered. In addition to European and American plain vanilla put and call options, there are other types of options that take into account different trading strategies [8].

In our paper we focus on American options. The holder of a put option exercises the option if $S<K$, since he can sell the predefined amount at the price $K\in\mathbb{R}^+$ instead of the market price for the underlying $S\in\mathbb{R}^+$. The exercise region of a put option is defined as the range in which a profit is gained, this is the region where $K-S>0$. If $K-S\leq 0$ the option will not be exercised, because exercising it would result in a loss. Similarly, a call option will be exercised in the $K<S$ region. These results are summarized in the payoff-function $\phi(S)$:

$$\phi(S)=\begin{cases}\max(S-K,0)=(S-K)^+ & \text{for} \quad S\geq 0 \quad \text{(Call)},\\ \max(K-S,0)=(K-S)^+ & \text{for} \quad S\geq 0 \quad \text{(Put)},\end{cases} \tag{1.1}$$

with the abbreviation $(\cdot)^+=\max(\cdot,0)$. Since American options can be exercised before the maturity, the trading strategy is to exercise the option on the unknown time point before or at maturity, where $K-S>0$ is maximal. Therefore the time dependent free boundary value $S_f(t)$ is introduced and for the price of a American Put option $P(S,t)$ holds

$$\begin{aligned} &P(S,t)=\phi(S)=(K-S)^+=K-S && \text{for} \quad S\leq S_f(t),\\ &P(S,t)>\phi(S)=(K-S)^+ && \text{for} \quad S>S_f(t).\end{aligned}$$

The dynamics of the price of the underlyings can be described via a stochastic differential equation (SDE) which corresponds to a partial differential equation (PDE). In 1973 Black and Scholes developed the Black-Scholes model [1], where the dynamic is described by

$$\frac{dS_t}{S_t}=rdt+\sigma dW_t^S, \tag{1.2}$$

where r is the constant interest rate, σ is the constant variance and dW_t^S denotes a Brownian motion. Starting from this SDE, we obtain the price of an American Put Option $P(S,t)$ by solving the partial differential equation

$$P(S,t)=\frac{\partial V}{\partial t}+\frac{1}{2}\nu S^2\frac{\partial^2 V}{\partial S^2}+rS\frac{\partial V}{\partial S}-rV\geq 0, \quad S>0, \quad 0<t\leq T. \tag{1.3}$$

Since ν and r are non-constant parameters in the real market as well, until now several extension have been developed to gain more flexibility and comparability to real market situations. Some extensions consider nonlinear functions, e.g., for σ resulting in nonlinear Black-Scholes models [6], other extensions include an additional SDE, e.g., a stochastic volatility or a stochastic interest rate [11, 27]. In the sequel we discuss the Heston

model [13] that extended the Black Scholes model by adding a Cox-Ingersoll-Ross (CIR) process for modelling the stochastic volatility.

This paper is structured as follows. Section 2 introduces the concept of American options and the Heston model. In Section 3 the spatial approximation by sparse grids and the combination technique is motivated and described. For the temporal discretization the well-known ADI methods are considered in Section 4. In Section 5 the results are presented and discussed. The paper finishes with a conclusion and an outlook on future research aspects.

2 American put options under the Heston model

For American Options the payoff function $\phi(S)$ for the price of the underlying $S>0$ with respect to the predefined strike $K\in\mathbb{R}^+$ at the exercise date is given by (1.1). For the pricing of an American put option P we look for the solution P and the associated free boundary S_f, i.e., the tuple $\big(P(S,t),S_f(t)\big)$ such that

$$P(S,t)=\phi(S) \qquad \text{for } S\leq S_f(t), \tag{2.1a}$$

$$P(S,t)>\phi(S) \qquad \text{for } S>S_f(t), \tag{2.1b}$$

where S denotes the price of an asset at time t with $0\leq t\leq T$.

In the following, we consider the two-dimensional Heston model to describe the dynamics of the price S. The system of SDEs under a risk neutral measure for the Heston model is

$$\begin{cases} dS_t = rS_t dt+\sqrt{v_t}S_t dW_t^S, & S_0>0,\\ dv_t = \kappa_v(\mu_v-v_t)dt+\sigma_v\sqrt{v_t}dW_t^v, & v_0>0, \end{cases} \tag{2.2}$$

where $v>0$ is the square of the volatility of the underlying, κ_v is the mean-reversion rate and μ_v is the long-term mean of the volatility v and σ_v is the volatility-of-variance. The

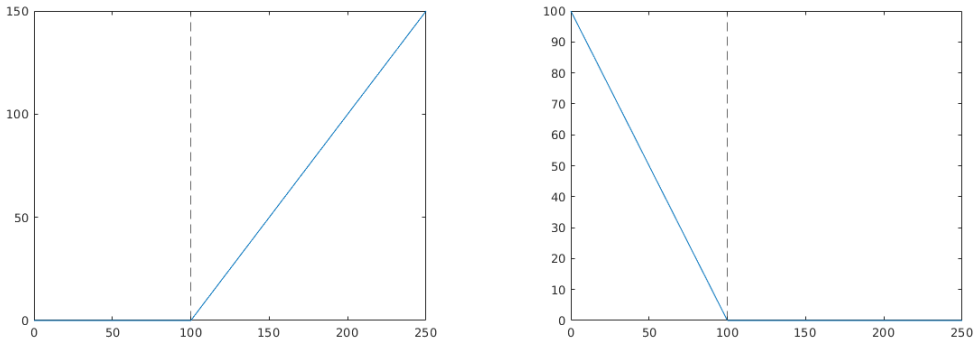

(a) Payoff function for a Call option (b) Payoff function for a Put option

Figure 1: Payoff function for $S\in[0,250]$ with $K=100$, where the dashed line markes the strike.

SDE processes are driven by the Brownian motions W_t^S and W_t^ν which are correlated by a constant parameter $\rho\in[-1,1]$. If the Feller condition $2\kappa_\nu\mu_\nu>\sigma_\nu$ is fulfilled, $\nu>0$ applies. In order to derive a PDE from the SDE system (2.2) under a risk neutral measure, Itô's Lemma or Kolmogorov's backward equation is used. The resulting differential operator for the fair price of an American put option $P(S,\nu,t)$ is given by

$$\mathcal{L}_H[P]=\frac{1}{2}\nu S^2\frac{\partial^2 P}{\partial S^2}+\rho_{S\nu}\sigma_\nu S\nu\frac{\partial^2 P}{\partial S\partial\nu}+\frac{1}{2}\sigma_\nu^2\nu\frac{\partial^2 P}{\partial\nu^2}+rS\frac{\partial P}{\partial S}+\kappa_\nu(\nu-\mu_\nu)\frac{\partial P}{\partial\nu}-rP. \tag{2.3}$$

The terminal condition at the expiry date $t=T$ reads

$$P(S,\nu,T)=\phi(S),\quad S>S_f(T), \tag{2.4}$$

the spatial boundary conditions for S are given by

$$P(0,\nu,t)=K,\quad \lim_{S\to\infty}P(S,\nu,t)=0,\quad 0\le t\le T, \tag{2.5}$$

for the boundaries $\nu=0$ and $\nu=\nu_{\max}$, the equation

$$\frac{\partial P}{\partial\tau}-\mathcal{L}_H[P]=0$$

has to be fulfilled. The "spatial" boundary conditions at $S=S_f(t)$, $S\to\infty$ are given by

$$P\big(S_f(t),\nu_f(t),t\big)=\phi(S_f(t)),\quad \frac{\partial P}{\partial S}\big(S_f(t),\nu_f(t),t\big)=-1,\quad 0\le t\le T. \tag{2.6}$$

In order to solve a forward-in-time PDE, we utilize the time reversal $\tau=T-t$ and the differential operator has to fulfill the inequality

$$\frac{\partial P}{\partial\tau}-\mathcal{L}_H[P]\le 0. \tag{2.7}$$

We recast the American option problem into a linear complementary problem (LCP)

$$\begin{cases}\big(P-\phi(S)\big)\cdot\left(\dfrac{\partial P}{\partial\tau}-\mathcal{L}_H[P]\right)=0,\\ -\left(\dfrac{\partial P}{\partial\tau}-\mathcal{L}_H[P]\right)\ge 0,\\ P-\phi(S)\ge 0,\end{cases} \tag{2.8}$$

and apply an operator splitting [17]. The reformulation of the LCP with an auxiliary variable λ is given by

$$\begin{cases}\mathcal{L}_H[P]-\dfrac{\partial P}{\partial\tau}=\lambda,\\ \lambda\ge 0,\quad P-\phi(S)\ge 0,\quad \big(P-\phi(S)\big)\lambda=0,\end{cases} \tag{2.9}$$

for $(S,\nu,\tau)\in\Omega\times[0,T]$ with the initial and boundary conditions [18]. It results in a mixed formulation of the LCP problem, where λ plays the role of a Lagrange multiplier. The advantage of the LCP formulation of American Option problems is that an explicit computation for the free boundary value $S_f(\tau)$ is avoided.

3 Sparse grids

In the field of computational finance, we are looking for new ways to reduce memory space and runtime as models become more complex, and we strive for higher stability and accuracy as run-time and memory space increase with the amount and size of the dimension of the models. To reduce the computational effort, splitting methods, e.g., ADI schemes, have been considered. However, these are also limited by memory space, since the increase in computational effort depends on the number of grid points, e.g., a d-dimensional full-tensor based grid contains $\mathcal{O}(N^d)$ nodes. Therefore, in the literature [2, 4, 7, 21] other grid structures such as multigrid methods and sparse grids have been introduced.

In the following, we focus on the sparse grid approach using the combination technique to reduce the effects of increasing the dimension. Sparse grids were developed by Smolyak [24] for numerical integration purposes. Later the approach was extended in [2, 22, 23, 28] and in 2015 Hendricks et al. [12] introduced the approach for financial applications.

3.1 The spatial grid

We consider a 2-dimensional domain Ω_2 in a continuous setting, where $x \in \Omega_2$. With the help of the multi-indices $l = (l_1, l_2) \in \mathrm{N}_0^2$, $j = (j_1, j_2) \in \mathrm{N}_0^2$, $N = (N_1, N_2) = (2^{l_1}, 2^{l_2})$, we can define a tensor based grid Ω_l with grid nodes

$$x_{l,j} = (y_{l_1,j_1}, z_{l_2,j_2}) \quad \text{for} \quad j_1 = 0,1,\cdots,\mathrm{N}_1 \quad \text{and} \quad j_2 = 0,\cdots,\mathrm{N}_2, \tag{3.1}$$

where the value x_{l_i,j_i} denotes the position in the i-th coordinate of the j_i-th node. For a fixed l on $\Omega_2 = [0,1]^2$, we set $x = (y,z)$ and obtain a uniform grid with mesh width $h = (2^{-l_1}, 2^{-l_2})$. To reconstruct a nonuniform grid for the spatial variables S and ν, we consider a smooth transform function. The transformation is only shown for S, since the transformation for ν is similar. We introduce the transformation function

$$y = \psi(S) \tag{3.2}$$

on the arbitrary interval $[y_{\min}, y_{\max}] = [0,1]$ with $S_{\min}, S_{\max} \in \mathbb{R}$ and $S_{\min} < S_0 < S_{\max}$

$$\psi^{-1}(y) = S_0 + \alpha \cdot \sinh(y \cdot (c_2 - c_1) + c_1), \tag{3.3a}$$

$$c_1 = \sinh^{-1}\left(\frac{S_{\min} - S_0}{\alpha}\right), \qquad c_2 = \sinh^{-1}\left(\frac{S_{\max} - S_0}{\alpha}\right). \tag{3.3b}$$

Small α values lead to highly non-uniform grids, while large values of α lead to a uniform distribution of grid points [19,25]. For the transformation for the asset S a common choice is $S_{\min} = 0$, $S_{\max} = 3K$ and $S_0 = K$. For accuracy purpose, we choose $S_0 = \tilde{S}$, where $\tilde{S}$ is the spot asset price for the American put option. Since the initial condition processes a

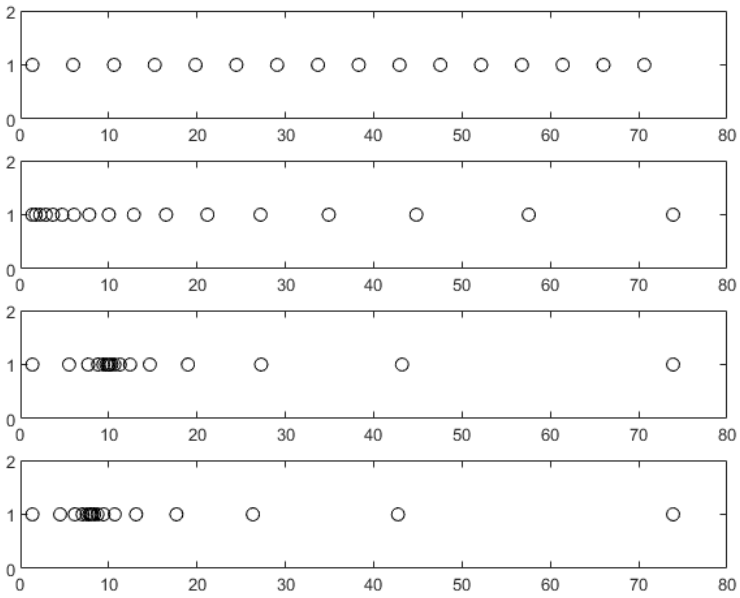

Figure 2: Different transformations for $S\in[K\cdot\exp(-2),K\cdot\exp(2)]$ with 17 discrete points, with $K=10$. The first distribution is a uniform discretization on S, the second shows $S=K\exp(\hat{S})$ with $\hat{S}_{\min}=-2$ and $\hat{S}_{\max}=2$. The third and fourth distribution show the transformation with Eq. (3.2) and $\alpha=0.25$, where in the third $S_0=K$ is chosen and in the last $S_0=\tilde{S}=8$.

discontinuous derivative at K, this choice avoids numerical difficulties with nonsmooth data. The operator for the transformed Heston PDE reads

$$\begin{aligned}\mathcal{L}[P]=&\frac{1}{2}\nu S^2a_S^2\frac{\partial^2P}{\partial y^2}+\left(rSa_S+\frac{1}{2}\nu S^2b_S\right)\frac{\partial P}{\partial y}+\rho a_Sa_\nu\sigma S\nu\frac{\partial^2P}{\partial y\partial z}\\&+\frac{1}{2}\sigma^2\nu a_\nu^2\frac{\partial^2P}{\partial z^2}+\left(\kappa(\nu-\mu)a_\nu+\frac{1}{2}\sigma^2\nu b_\nu\right)\frac{\partial P}{\partial z},\end{aligned}\tag{3.4}$$

where

$$a_S=\frac{\partial\psi(S)}{\partial S},\quad b_S=\frac{\partial^2\psi(S)}{\partial S^2},$$

and a_ν and b_ν analogously. Usually in finance the transformation $\hat{S}=\ln(S/K)$ is used. A comparison of the grid transformations is shown in Fig. 2.

3.2 The sparse grid combination technique

To introduce the sparse grid combination technique, we follow the approach of Reisinger [22]. Due to the grid transformation we obtain the grid domain $\Omega_2=[0,1]^2$. The solution P_l is

defined on Ω_l with $l=(l_1,l_2)\in\mathbb{N}_0^2$ with the mesh width $h=(h_1,h_2)=(2^{-l_1},2^{-l_2})$. To use the combination technique, we consider the error splitting

$$P-P_l=h_1^2w_1(h_1)+h_2^2w_2(h_2)+h_1^2h_2^2w_{1,2}(h_1,h_2), \tag{3.5}$$

where w_1 only depends on h_1, w_2 only on h_2 and h_1 and h_2 are independent from each other. Each of w_1, w_2, $w_{1,2}$ is bounded. The next step is to define a *hierarchical surplus*

$$\delta(P_l)=P_l-P_{l-e_1}-P_{l-e_2}-P_{l-e_1-e_2},\quad e_1=(1,0),e_2=(0,1), \tag{3.6}$$

and by inserting it into the error splitting, we obtain

$$\begin{aligned}\delta(P-P_l)=&h_1^2h_2^2w_{1,2}(h_1,h_2)-4h_1^2h_2^2w_{1,2}(2h_1,h_2)\\&-4h_1^2h_2^2w_{1,2}(h_1,2h_2)+16h_1^2h_2^2w_{1,2}(2h_1,2h_2)\\=&\mathcal{O}(2^{-2|l|_1}).\end{aligned} \tag{3.7}$$

Note that the surplus can be interpreted as information gain of the solution P_l and that the solution on the discrete grid Ω_l given by $|l|_1$ with the same number of grid nodes have the same surplus. The combination technique is motivated by getting the highest information gain from the sub-solutions with high information gain, with a high surplus. Therefore we define the combined sparse grid solution as the sum of all surpluses with $|l|_1\leq n$ for $n\in\mathbb{N}_0$

$$P_n^s=\sum_{|l|_1\leq n}\delta P_l=\sum_{|l|_1=n}P_l-\sum_{|l|_1=n-1}P_l. \tag{3.8}$$

An upper error bound can be found by incorporating the surpluses of all sub-solutions, with $|l|_1<n$

$$||P_n^s-P||\leq\mathcal{O}\left(h^2\log_2(h^{-1})\right). \tag{3.9}$$

A close look into the sub-solutions within the combined sparse grid solution shows that the sparse grid combination formula at level $n\in\mathrm{N}$ is given by

$$P_n^s=\sum_{|l|_1=n}P_l-\sum_{|l|_1=n-1}P_l. \tag{3.10}$$

We observe that all sub-solutions with $|l|_1<n-1$ cancel out. Fig. 3 shows that the sparse grid solution contains also highly disordered grids. In order to avoid numerical instability due to sensitivities to it, we set a minimum mesh width in our numerical experiments with $l_i\geq l_{\min}$ for $i=1,2$. To have at least 9 grid points in each dimension, we set $l_{\min}=3$. Since numerical experiments for the Heston model have given evidence that for efficiency reasons, it is sufficient to use only half of the spatial grid points in the volatility direction than in the asset direction: $N_1=N_2/2$, cf. [9]. Therefore we introduce an additional condition for l, which results in a reduced grid resolution in volatility direction.Due to the special setting for the grid points where the number of grid points is given by $(N_1,N_2)=(2^{l_1},2^{l_2})$, we can easily adapt the restriction for number of grid points for the volatility, by setting $l_1>l_2$.

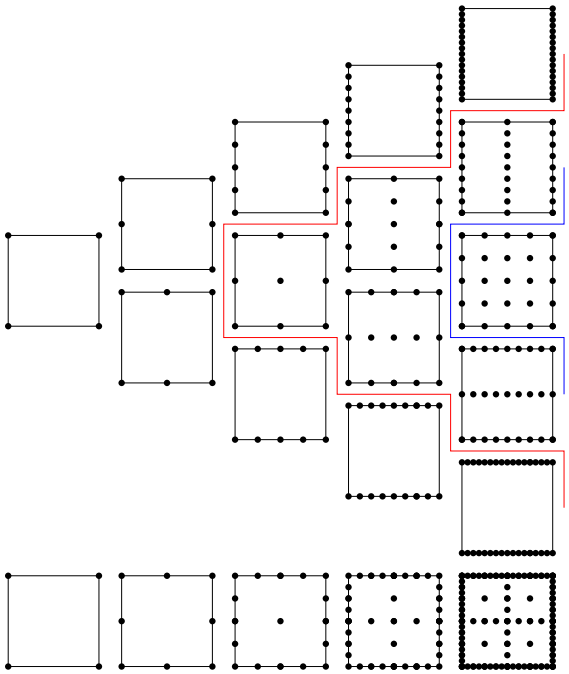

Figure 3: Subgrids and corresponding sparse grids for $|l|_1 = 0,1,2,3,4$. The separating line starting between the second and thrid row includes all grids with $l_{\min} = 2$ and the other seperating line starting before the last row includes all sub-grids with $l_{\min} = 3$.

3.3 The finite difference method

For the approximation of the spatial derivatives we use second order finite differences. We introduce $y \in [0,1]$ and $z \in [0,1]$ and consider a uniform grid for y and z, due to the choice of α we obtain a highly non-uniform lattice of S and v with grid points concentrated around S_0 and v_0, see Fig. 2. Since we use sparse grids, we solve the Heston PDE on several different grids by using the same spatial approximations for the derivatives, namely central difference quotients of order two in each direction. In addition, we consider the forward and backward difference quotients of second order at the boundaries. Note that the mixed derivative at the boundaries for $z = 0$ is zero, as is the diffusion term, so it is treated trivially. An improvement in accuracy can be achieved by using higher order stencils within the finite difference methods (FDMs) or by considering spectral methods. In [10], it is shown that higher order stencils have a higher gain than the spectral methods. Furthermore, switching between different stencils in the FDM is easier to adjust than using a new method, e.g., spectral methods.

The spatial discretization leads to an approximation of the option value $P(y,z,\tau)$ at the spatial grid points $(y,z) \in [0,1]$ for an LCP, analogously to (2.9), for the transformed

operator $\mathcal{L}$. For $0<\tau<T$, the solution vector $P(\tau)$ of the semi-discrete partial differential complementary problem (PDCP)

$$\frac{\partial P}{\partial \tau}=FP(\tau)+\lambda(\tau),\quad P(\tau)\geq\phi\big(\psi^{-1}(y)\big),\quad \Big(P(\tau)-\phi\big(\psi^{-1}(y)\big)\Big)^{\top}\lambda(\tau)=0, \tag{3.11}$$

gives an approximations for $P(x,y,\tau)$. The inequalities are component wise and F is a given real matrix, where $\phi(S)$ is the initial condition.

4 Alternating direction implicit methods

For the temporal discretization, we set $\Delta\tau=T/N_t$ with $N_t\geq 1$ and obtain $\tau_k=k\cdot\Delta\tau$ for $k=0,\cdots,N_t$. Let u^k be the discrete solution for the transformed solution $P(y,z,\tau_k)$ at time step k and g the discrete payoff values. Once a time discretization is applied to the PDCP (3.11), we obtain a fully discretized LCP of the form

$$\begin{cases} u^{k+1}=Fu^k+\Delta\tau\lambda^{k+1}, & (4.1)\\ \lambda^{k+1}\geq 0,\quad u^{k+1}\geq g,(\lambda^{k+1})^{\top}(u^{k+1}-g), & (4.2)\end{cases}$$

where $F\in\mathbb{R}^{(\mathbb{N}_1+1)(\mathbb{N}+1)\times(\mathbb{N}_1+1)(\mathbb{N}+1)}$ are discretization matrices and $\lambda\in\mathbb{R}^{(\mathbb{N}_1+1)(\mathbb{N}+1)}$ is the auxiliary term and u^k approximates $P(y,z,\tau_k)$ [17, 18, 20]. In the first fractional step (4.1) a system of linear equations is solved. The system of equations depends on the chosen time discretization method, which is in our case the alternating direction implicit (ADI) method. These ADI methods are often used in financial applications, cf. [9, 10, 19, 20], to split the operator of the multidimensional PDE into separate operators corresponding to the directions. Let I denote the identity matrix and $\mathcal{A}_y$ be the approximation for the first derivative to y, analogously we introduce $\mathcal{A}_{yy}$, $\mathcal{A}_z$, $\mathcal{A}_{zz}$ and $\mathcal{A}_{yz}$. We define

$$\mathcal{F}_0(\tau,u)=\rho a_S a_\nu\sigma S\nu\mathcal{A}_{yz}u(\tau), \tag{4.3a}$$

$$\mathcal{F}_1(\tau,u)=\left(\frac{1}{2}\nu S^2a_S^2\mathcal{A}_y+\left(rSa_S+\frac{1}{2}\nu S^2b_S\right)\mathcal{A}_{yy}-\frac{1}{2}rI\right)u(\tau), \tag{4.3b}$$

$$\mathcal{F}_2(\tau,u)=\left(\frac{1}{2}\sigma^2\nu a_\nu^2\mathcal{A}_z+\left(\kappa(\nu-\mu)a_\nu+\frac{1}{2}\sigma^2\nu b_\nu\right)\mathcal{A}_{zz}-\frac{1}{2}rI\right)u(\tau), \tag{4.3c}$$

$$\mathcal{F}(\tau,u)=\sum_{i=0}^{2}\mathcal{F}_i(\tau,u). \tag{4.3d}$$

The matrices $\mathcal{F}$ have a small bandwidth up to permutations. The four well-known ADI schemes are the Douglas (DO) scheme [5], the Craig-Sneyd (CS) scheme [3], the modified Craig-Sneyd (mCS) scheme [3] as well as the Hundsdorfer-Verwer (HV) scheme [16], presented below. Further let $\theta>0$ be a given real parameter depending on the stability constraints of the method, we choose $\theta=0.5$ for DO and CS, $\theta=\frac{1}{3}$ for mCS and $\theta=\frac{1}{2}+\frac{1}{6}\sqrt{3}$,

cf. [14, 15, 19]. As an American option problem includes an inequality, we further have to add the additional auxiliary term λ to the classical ADI approach in each time step, cf. [9, 17]. Exemplary, the term written in a box will be added to the Douglas-Scheme. The Douglas scheme with λ is given by

$$\begin{cases} Y_0 = u^k + \Delta\tau \mathcal{F}(\tau^k, u^k) \boxed{+\Delta\tau\tilde{\lambda}^{k+1}}, \\ Y_i = Y_{i-1} + \theta\Delta\tau(\mathcal{F}_i(\tau^{k+1}, Y_i) - \mathcal{F}_i(\tau^k, u^k)) \quad \text{for } i = 1, \cdots, d, \\ \tilde{u}^{k+1} = Y_d. \end{cases} \tag{4.4}$$

The second fractional step (4.2) updates the λ^k and u^k such that they satisfy the constraints in each time step [9, 18]. The update step can easily solved component wise by

$$u^{k+1} = \max(\tilde{u}^{k+1} - \Delta\tau\lambda^k, u^0), \quad \lambda^{k+1} = \max(0, \lambda^k + (u^0 - \tilde{u}^{k+1})/\Delta\tau). \tag{4.5}$$

Since we have an initial condition, we set λ^0 as the zero vector. The vector $\tilde{\lambda}^{k+1}$ is an approximation of λ^{k+1}, which is can be estimated by $\tilde{\lambda}^{k+1} = \lambda^k$ or by linear extrapolation to a non-uniform grid

$$\tilde{\lambda}^{k+1} = \lambda^k + \frac{\Delta\tau^{k+1}}{\Delta\tau^k}(\lambda^k - \lambda^{k-1}). \tag{4.6}$$

To reduce memory space and run-time, we use a more intelligent implementation with the same stability and accuracy as the naive implementation [26].

5 Results

In this section we numerically investigate the behaviour of the schemes in connection with our extensions. First, we focus on the analysis of the limitation for the number of grid points in the sparse grids. Therefore we consider the parameter set

$$T = 0.25, \quad K = 10, \quad \kappa = 5, \quad \mu = 0.16, \quad \sigma_\nu = 0.9, \quad \rho = 0.1, \quad r = 0.1. \tag{5.1}$$

For the sparse grid structure for y and z, we set $|l|_1 = 9$, $l_{\min} = 3$. For the grid transformation to S and ν, we choose $S_{\min} = 0$, $S_0 = \tilde{S}$ and $S_{\max} = 3K$ as well as $\nu_{\min} = 0$, $\nu_0 = \tilde{\nu}$ and $\nu_{\max} = 3$; further $\alpha_S = \alpha_\nu = 2$. For the different ADI methods, $N_t = 100$ and θ are selected as in Section 4. This parameter set fulfils the Feller condition and is widely used in the literature, cf. [4, 9, 18, 21]. Since Haentjens and in't Hout [9] also solved this example set with ADI methods, but on a full grid structure, we compare our results with their solution. The accuracy of the model is shown in Table 1. Our solution of this test set was calculated without smoothing the initial data, since we use the spot price for the grid transformation. As expected, the results obtained from the limited sparse grid setting are in the same accuracy range as the common set, the main advantage of the limitation is the shortening of the run-time. For the comparison of the run-time between the

Table 1: Solution values for the different spot asset prices and spot volatility's for the parameter set (5.1).

$\tilde{v}=0.0625$					
$\tilde{S}$	8	9	10	11	12
[9]	2.0000	1.1081	0.5204	0.2143	0.0827
without Limitation					
DO	2.0011	1.1095	0.5203	0.2131	0.0821
CS	2.0011	1.1095	0.5202	0.2131	0.0820
mCS	2.0011	1.1093	0.5199	0.2129	0.0821
HV	2.0012	1.1101	0.5215	0.2136	0.0818
with Limitation					
DO	2.0006	1.1085	0.5176	0.2132	0.0821
CS	2.0006	1.1085	0.5176	0.2131	0.0820
mCS	2.0005	1.1083	0.5172	0.2130	0.0821
HV	2.0005	1.1091	0.5188	0.2136	0.0816

$\tilde{v}=0.25$					
$\tilde{S}$	8	9	10	11	12
[9]	2.0788	1.3339	0.7962	0.4486	0.2433
without Limitation					
DO	2.0787	1.3339	0.7962	0.4481	0.2430
CS	2.0787	1.3338	0.7961	0.4481	0.2430
mCS	2.0785	1.3334	0.7956	0.4476	0.2427
HV	2.0792	1.3346	0.7928	0.4371	0.2415
with Limitation					
DO	2.0786	1.3336	0.7961	0.4483	0.2431
CS	2.0786	1.3336	0.7961	0.4483	0.2430
mCS	2.0783	1.3331	0.7955	0.4479	0.2428
HV	2.0791	1.3343	0.7935	0.4368	0.2270

full sparse grid and the reduced sparse grid, we compute a reference solution with the Crank-Nicolson scheme and initial data smoothing. Further we discretize to a grid with $(129,33)$ grid points and 10,000 time steps with a second-order stencil. Fig. 4 shows the effect of the reduction of the grid resolution in the volatility direction on the run-time for sparse grid settings for the test set (5.1) in comparison with the accuracy. We used Julia as computation language and run the computations on an Intel(R) Core(TM) i7-8700K CPU @ 3.70 GHz. Note that the intelligent implementation of the ADI schemes [26] already reduces the run-time once.

6 Conclusions

In this paper we have shown that the numerical results of the grid transformation on the spot price with the reduced resolution in the direction of volatility are satisfactory even

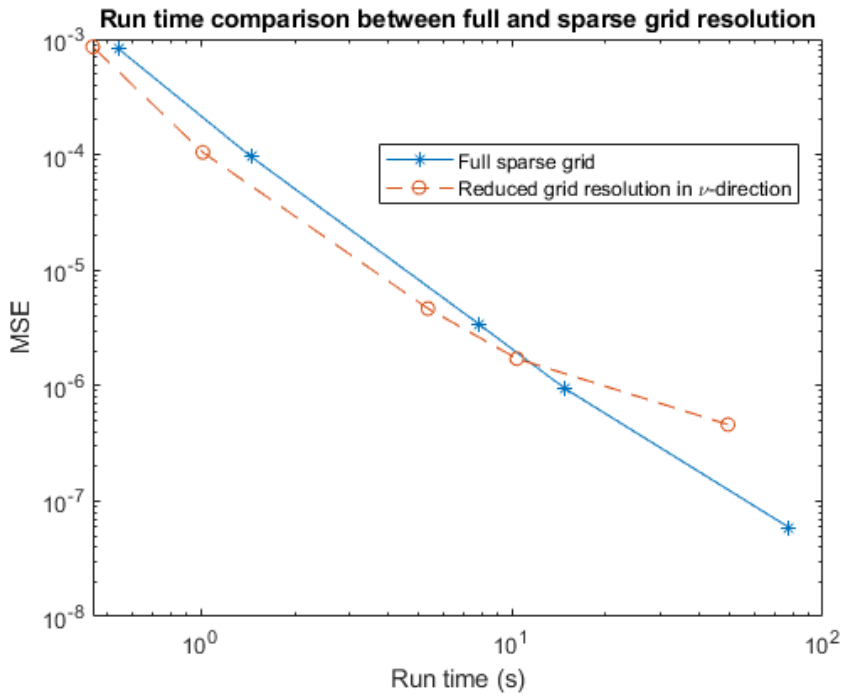

Figure 4: Run-time comparison between the sparse grid solution with and without limitation for the parameter set (5.1). The run time of mCS is shown, where the line with the star represents the run-time of the sparse grid solution without any limitation and the dashed line with the circles corresponds to the run-time for the sparse grid with reduced grid resolution.

without smoothing. As in this setting, the best improvement was achieved in using the spot price as the accumulation point of the transformation (instead of the strike price). Furthermore, we have achieved a runtime improvement due to the reduced grid resolution in the direction of volatility, even though we have already worked on a sparse grid structure and runtime-optimized implementations. In summary, the paper shows different ways to further improve known methods in order to adapt the time requirements.

Acknowledgements

The work of the authors was partially supported by the bilateral German-Slovakian Project MATTHIAS–Modelling and Approximation Tools and Techniques for Hamilton-Jacobi-Bellman equations in finance and Innovative Approach to their Solution, financed by DAAD and the Slovakian Ministry of Education. Further the authors acknowledge partial support from the bilateral German-Portuguese Project FRACTAL–FRActional models and CompuTationAL Finance financed by DAAD and the CRUP–Conselho de Reitores das Universidades Portuguesas.

References

[1] F. BLACK AND M. SCHOLES, *The pricing of options and corporate liabilities,* J. Polit. Econ., 81(3) (1973), pp. 637–654.

[2] H. BUNGARTZ AND M. GRIEBEL, Sparse Grids, Cambridge University Press, 2004, pp. 1–123.

[3] I. J. D. CRAIG AND A. D. SNEYD, *An alternating-direction implicit scheme for parabolic equations with mixed derivatives,* Comput. Math. Appl., 16(4) (1988), pp. 341–350.

[4] N. CLARKE AND K. PARROTT, *The multigrid solution of two factor American put options,* Research Report 96-16, Oxford Computing Laboratory, Oxford 1996.

[5] J. DOUGLAS AND H. RACHFORD, *On the numerical solution of heat conduction problems in two and three space variables,* Trans. Amer. Math. Soc., 82 (1956), pp. 421–439.

[6] M. EHRHARDT, Nonlinear Models in Mathematical Finance, New Research Trends in Option Pricing, New York: Nova Science Publishers, 2018.

[7] J. FRANK AND W. HUNDSDORFER, *On the stability of implicit-explicit linear multistep methods,* Appl. Numer. Math., 25(2-3) (1997), pp. 193–205.

[8] M. GÜNTHER AND A. JÜNGEL, Finanzderivate mit Matlab. Mathematische Modellierung und Numerische Simulation, Vieweg+Teubner Verlag, Wiesbaden, 2 edition, (2010).

[9] T. HAENTJENS AND K. J. IN'T HOUT, *ADI schemes for pricing American options under the Heston model,* Appl. Math. Fin., 22 (2013), pp. 207–237.

[10] C. HENDRICKS, C. HEUER, M. EHRHARDT AND M. GÜNTHER, High-Order-Compact ADI Schemes for Pricing Basket Options in the Combination Technique, Chapter in: M. Ehrhardt, M. Günther and J. ter Maten, (eds.), Novel Methods in Computational Finance, Springer, 2017.

[11] C. HENDRICKS, M. EHRHARDT AND M. GÜNTHER, *Hybrid finite difference/pseudospectral methods for the Heston and Heston-Hull-White PDE,* J. Comput. Finance, 21(5) (2018), pp. 1–33.

[12] C. HENDRICKS, M. EHRHARDT AND M. GÜNTHER, *High-Order ADI schemes for diffusion equations with mixed derivatives in the combination technique,* Appl. Numer. Math., 101 (2016), pp. 36–52.

[13] S. L. HESTON, *A closed-form solution for options with stochastic volatility with applications to bond and currency options,* Rev. Financial Studies, 6 (2) (1993), pp. 327–343.

[14] W. HUNDSDORFER, *A note on stability of the Douglas splitting method,* Math. Comput., 67(221) (1998), pp. 183–190.

[15] W. HUNDSDORFER, *Stability of Approximate Factorization with θ-methods,* BIT Numer. Math., 39(3) (1999), pp. 473–483.

[16] W. HUNDSDORFER, *Accuracy and stability of splitting with stabilizing corrections,* Appl. Numer. Math., 42(1-3) (2002), pp. 213–233.

[17] S. IKONEN AND J. TOIVANEN, *Operator splitting methods for pricing American options under stochastic volatility,* Numer. Math., 113(2) (2009), pp. 299–324.

[18] S. IKONEN AND J. TOIVANEN, *Operator splitting methods for American option pricing,* Appl. Math. Lett., 17(7) (2004), pp. 809–814.

[19] K. J. IN'T HOUT AND S. FOULON, *ADI finite difference schemes for option pricing in the Heston Model with correlation,* Int. J. Numer. Anal. Mod., 7 (2010), pp. 303–320.

[20] K. J. IN'T HOUT AND J. TOIVANEN, Application of Operator Splitting Methods in Finance, in: R. Glowinski, S. Osher, W. Yin (eds.), Splitting Methods in Communication, Imaging, Science, and Engineering, Scientific Computation, Springer, Cham, 2016, pp. 541–575.

[21] C. W. OOSTERLEE, *On multigrid for linear complementarity problems with application to American-style options,* Elec. Trans. Numer. Anal., 15 (2003), pp. 165–185.
[22] C. REISINGER, *Analysis of linear difference schemes in sparse grid combination technique,* IMA J. Numer. Anal., 33(2) (2013), pp. 544–581.
[23] T. SCHIEKOFER, Die Methode der Finiten Differenzen auf dünnen Gittern zur Lösung elliptischer und Parabolischer Partieller Differentialgleichungen, PhD thesis, Universität Bonn, 1999.
[24] S. SMOLYAK, *Quadrature and interpolation formulas for tensor products of certain classes of functions,* Dokl. Akad. Nauk SSSR, 148 (1963), pp. 1042–1045.
[25] D. TAVELLA AND C. RANDALL, Pricing Financial Instruments: The Finite Difference Method, Wiley, New York, 2000.
[26] L. TENG AND A. CLEVENHAUS, *Accelerated implementation of the ADI schemes for the Heston model with stochastic correlation,* J. Comput. Sci., 36 (2019), 101022.
[27] L. TENG, M. EHRHARDT, M. GÜNTHER, *Numerical simulation of the Heston model under stochastic correlation,* Int. J. Financial Studies, 6 (2017), pp. 3.
[28] C. ZENGER, Sparse Grids, Technical Report, Institut für Informatik, Technische Universität München, October 1990.